Research Article

# Green synthesis of silver nanoparticles using *Eulophia herbacea* (Lindl.) tuber extract and evaluation of its biological and catalytic activity

**Jayashri S. Pawar**[1] · **Ravindra H. Patil**[1]

Received: 11 September 2019 / Accepted: 4 December 2019 / Published online: 9 December 2019


**Abstract**
The present work is a report on phytosynthesis of silver nanoparticles (AgNPs) carried out using an aqueous extract of the tuber of *Eulophia herbacea* Lindl. (Orchidaceae) and evaluation of its antimicrobial and catalytic potential. The extract efficiently reduced aqueous silver ions and generated stable and bioactive nanoparticles. The maximum reduction of $AgNO_3$ was achieved when 1 mM $AgNO_3$ was incubated with 2% w/v extract for 5 h. The biosynthesized AgNPs exhibited surface plasma resonance at 447 nm. The zeta potential was − 15 mV. Scanning electron microscopy study showed that the average particle size of the AgNPs was 11.70 ± 2.43 nm and that they were non-agglomerated. An Energy Dispersive X-ray study provided support for the presence of elemental silver. X-ray diffraction studies confirmed that the AgNPs were crystalline and had a face-centered cubic geometry. The AgNPs showed excellent antibacterial and antifungal activity against common human pathogens. This activity was comparable with that of standard antibiotics. The catalytic potential of the AgNPs was studied through the reduction of methylene blue and congo red. The results showed that the AgNPs synthesized using the present method are biologically and catalytically active.

**Keywords** *Eulophia herbacea* · Silver nanoparticles · Antimicrobial activity · Antifungal activity · Synergistic effect · Dye reduction

## 1 Introduction

There is growing interest in greener synthesis of metal nanoparticles. Plant extracts have been used for nanoparticles synthesis as the process involved is simple, eco-friendly and cost-effective. Moreover, this process is reproducible and easily scaled up [1]. In comparison with microbial synthesis, phytosynthesis is rapid. It does not require aseptic conditions, and it yields stable nanoparticles [2, 3].

Indian traditional systems of medicine recommend the use of medicinal and aromatic plants for curing various human illnesses. Plant extracts containing phytoconstituents are biologically and pharmacologically active. Plant metabolites are known to be excellent reducing and capping agents that can be used to synthesize nanoparticles effectively within a short time [4–6].

The tubers of *Curcuma longa* [4, 7], sweet potato [8], *Dioscorea bulbifera*, *Dioscorea batatas*, *Dioscorea oppositifolia*, etc. are rich with different reducing and capping agents that generate stable metal nanoparticles [9–11].

Silver is known for its antimicrobial and medicinal properties [12, 13]. However, the antimicrobial effect of silver ions and its salts is limited and of short duration. These limitations can be overcome by using silver nanoforms, which are inert, stable and act as antimicrobial agents effectively [9, 14, 15].

Numerous mechanisms are involved in the microbicidal effect of silver nanoparticles (AgNPs) [16]: (a) AgNPs produce structural changes in the cell membrane by deposition on it

✉ Ravindra H. Patil, ravi_nmu@yahoo.co.in; Jayashri S. Pawar, jayashripatil59@gmail.com | [1]Department of Microbiology and Biotechnology, R. C. Patel Arts, Commerce and Science College, District Dhule, Shirpur, Maharashtra 425 405, India.

[17]; (b) AgNPs form free radicals [18]; (c) AgNPs release silver ions [19], which can interact with and inactivate the thiol groups of several active enzymes [20]; (d) Ag is a soft acid, whereas cells are considered as soft bases (soft acids react with soft bases) [21]; (e) AgNPs destroy the DNA of cells as DNA consist of sulfur and phosphorus, which are considered soft bases. AgNPs modulate signal transduction in bacteria [22]. Moreover, in combination with AgNPs, antibiotics have increased bactericidal effect [9, 23]. Organic synthetic dyes are widely used in the textile, paper, paint, plastic and pharma industries are pollutants that are harmful to the environment [24]. Biosynthesized nanoparticles can degrade organic dyes effectively [25–28].

In the current work, we are for the first time, reporting the bioreduction capability of *E. herbacea* tuber extract for biosynthesis of AgNPs. *Eulophia herbacea* Lindl. (family Orchidaceae) is also known as *kukkadkand* or *kutrikand* [29]. It is terrestrial herb with fleshy subglobose tubers. Qualitative phytochemical tests have shown that carbohydrates, amino acids, mucilage, tannins, steroids and triterpenoids present in the tubers [30]. A decoction of the tuber has been used in the treatment of spermatorrhoea and urinary complaints and to provide relief during menses [31]. Traditionally, the tubers of the plant have been used in the treatment of tumors of the scrofulous glands of the neck and cardiac problems. They have also been used as an aphrodisiac and an appetizer. They possess antioxidant effects [32]. The tubers contain glucomannan (50–60%), which is responsible for their hypolipidemic and hypoglycemic activity [33, 34]. The tubers of *Eulophia herbacea* are used to make salep, a well-known Turkish drink [35, 36]. However, to the best of our knowledge, no reports are available on AgNPs biosynthesis potential of *E. herbacea* tubers.

Many researcher reported plant-mediated biosynthesis of metal nanoparticles, but lacking attention towards mechanistic approach. In this study, the phytoconstituents of tuber extract responsible for biosynthesis were quantified. Moreover, the present method of AgNPs synthesis is simple, rapid, cost-effective and can be operated at room temperature. The process parameters for AgNP biosynthesis were optimized. The AgNPs were characterized using UV–visible spectrophotometry, FT-IR spectroscopy, XRD, EDX and SEM. The AgNPs were evaluated for their antimicrobial (antibacterial and antifungal) and catalytic activity (dye reduction activity).

## 2 Materials and methods

### 2.1 Materials

The silver nitrate ($AgNO_3$), sodium borohydride ($NaBH_4$), methylene blue (MB), congo red (CR) and solvents used were of analytical grade and were obtained from SD Fine Chemicals, Mumbai, and Loba, Mumbai. All the solutions and reagents were prepared using double-distilled water. The microorganisms used to study the antimicrobial activity, such as *Staphylococcus aureus* (NCIM-2079), *Escherichia coli* (NCIM-2065), *Bacillus subtilis* (NCIM-2063) and *Pseudomonas aeuroginosa* (NCIM-2200), and the fungi *Aspergillus niger* (NCIM-1196) and *Fusarium moniliforme* (NFCCI-2949) were obtained from the culture depository of the Department of Microbiology, R. C. Patel Arts, Commerce and Science College, Shirpur, Maharashtra, India.

### 2.2 Methods

#### 2.2.1 Plant material collection and extract preparation

Tubers of *E. herbacea*were collected from the Toranmal forest (latitude 21.545645° N, longitude 74.467531° E), Nandurbar District, Maharashtra, India, in July and August. They were collected using sterile polythene bags according to standard procedures and identified by an expert taxonomist. Mature tubers were sliced thinly and shade-dried for 2 weeks. The dried material was ground to make a coarse powder of uniform particle size. An extract of the tuber powder (2 g) was produced by boiling it in 100 ml of double-distilled water for 10 min. The extract was filtered through Whatman filter paper No. 1. The filtrate was used in the subsequent experiments. Qualitative phytochemical screening of the extract was performed using methods described previously [37, 38].

#### 2.2.2 Biosynthesis of AgNPs and optimization

The aqueous extract of the *E. herbacea* tubers was used as a reducing agent in the biosynthesis of AgNPs. In brief, 2.5 ml of the aqueous extract was added to 10 ml of 1 mM $AgNO_3$ in an Erlenmeyer flask. The reaction mixture was kept at room temperature for 5 h. The reaction was monitored by absorbance scanning (200–800 nm) at 1-h intervals using a UV–visible spectrophotometer (UV-1700, Shimadzu, Japan). After incubation, the test samples were centrifuged at 10,000 rpm for 20 min at room temperature. The process of centrifugation and redispersion in double-distilled water was repeated thrice to ensure better separation of nanoparticles. The pellet of nanoparticles was dried, and the powdered residue was used for further experimentation [9, 39].

The AgNP biosynthesis was optimized using varying concentrations of $AgNO_3$ and tuber extract with respect to time. In brief, different amounts of the aqueous extract of *E. herbacea* tubers (0.5 ml, 1.0 ml, 2.0 ml, 2.5 ml, 3.0 ml, 4.0 ml) and different concentrations of $AgNO_3$ (0.1 mM, 1 mM, 2 mM, 5 mM, 10 mM) were used, keeping all the

other experimental parameters constant. The samples were scanned in the UV–visible range upto 5 h.

## 3 Instrumentation

The surface plasma resonance of the synthesized AgNPs in the range 200–800 nm was recorded using a double-beam UV–visible spectrophotometer (Shimadzu 1700, Japan). An FT-IR study was performed using an FT-IR spectrometer (IRAffinity-1, Shimadzu, Japan). The diffuse reflectance scan (DRS) sampling method was used in the 4000–400 $cm^{-1}$ range.

The dynamic light scattering (DLS) method was used to obtain polydispersity index (PDI), particle size and zeta potential measurements of the AgNPs and the $AgNO_3$ solution. A Zetasizer ZS 90 (Malvern Instruments Ltd., Malvern, UK) was used in making the measurements.

A scanning electron microscope (JEOL JSM-5600, USA) with a resolution of 3.5 nm and an accelerating voltage in the range from 0.5 to 30 kV was used to study the surface morphology of the nanoparticles and determine their size.

Conductive tape (double-sided carbon tape) was affixed on a polished aluminum surface. The AgNPs were placed at the center of the carbon tape. Pressure was applied, and excess free particles were removed by blowing. The samples were held in a vacuum chamber for 1 h and were loaded on the SEM instrument. The specifications of the BrukerD8 X-ray diffractometer were the following: voltage, 40 kV; current, 30 mA; and CuKα wavelength, 1.54 Å for X-ray diffraction pattern of AgNPs.

## 4 Biological and catalytic activity of AgNPs

### 4.1 Antimicrobial activity

The antibacterial potential of the synthesized AgNPs was evaluated using the agar well diffusion method [40, 41]. An aliquot of about 0.1 ml of bacterial suspension ($10 \times 10^6$ CFU/ml approximately) of the test organisms (*E. coli, S. aureus, P. aeuroginosa, B. subtilis*) was aseptically spread on a nutrient agar plate. The wells were prepared on nutrient agar plate using a sterile (6 mm diameter) cork borer. The well filled with 50 µl of biosynthesized AgNPs (20 µg/ml), 1 mM $AgNO_3$, plant tuber extract (2% w/v) and a standard antibiotic, streptomycin (30 µg/ml) (positive control). The plates were incubated at 37 °C for 24 h. The antibacterial activity was evaluated by measuring the zone of inhibition (in millimeters) [39]. The minimum inhibitory concentration (MIC) of the AgNPs against the test organisms *E. coli, S. aureus*, *P. aruginosaginosa*, *and B. subtilis*, was determined using the agar well diffusion method [40, 41]. The lowest concentration of AgNPs that had a zone of inhibition was measured [42, 43].

The antifungal activity of the synthesized AgNPs was evaluated using the agar well diffusion method [44]. A spore suspension of the test fungi (approximately $7 \times 10^6$ spores/ml) was aseptically spread on the surface of potato dextrose agar plate. Wells were prepared using a sterile (6 mm diameter) cork borer. The wells were filled aseptically with 50 µl of AgNPs (25 µg/ml), 1 mM $AgNO_3$, plant tuber extract (2% w/v) and a standard antibiotic, amphotericin B (30 µg/ml) (positive control). These plates were incubated at 28 °C for 48 h. The antifungal activity was evaluated by measuring the zone of inhibition.

### 4.2 Synergistic effect of AgNPs with antibiotic

The effect of the biosynthesized AgNPs in combination with standard antibiotics, streptomycin and chloramphenicol, against Gram-positive and Gram-negative bacterial strains was tested using the well diffusion method. 0.1 ml of a 24-h old culture of the test organism (*E. coli*, *S. aureus*, *P. aeuroginosa*, *B. subtilis*) was aseptically spread on a nutrient agar plate. The prepared wells were aseptically filled with AgNPs with a standard antibiotic to obtain a final concentration of 30 µg/ml. The plates were then incubated at 37 °C for 24 h [9]. The antimicrobial activity was determined by measuring the zone of inhibition against the test organisms. Next, the diameters of the inhibition zones of the AgNPs, the antibiotic and the AgNPs with the antibiotic were determined by subtracting the diameter of the well from the diameters of the total inhibition zone. The synergistic effect was calculated using the following equation [9, 45]:

$$\text{Synergistic effect} = \left(B^2 - A^2\right)/A^2,$$

where $A$ = Zone of Inhibition (ZOI) of the antibiotic, $B$ = ZOI of the combination of the AgNPs and the antibiotic.

### 4.3 Catalytic activity

The catalytic activity of the biosynthesized AgNPs was studied by evaluating their ability to reduce dyes such as methylene blue (MB) and Congo red (CR) in the presence of sodium borohydride [25, 46].

About 10.0 ml of MB (10 mM) was mixed with 2.0 ml of the AgNPs (7 µg/ml) and 1.0 ml of a 0.5 M ethanolic solution of sodium borohydride to determine the MB reduction activity. About 10.0 ml of a 1 mM solution of CR was added to 1 ml of an ethanolic borohydride solution and 1.0 ml of the AgNPs (7 µg/ml). The solution was mixed. From each of these solutions, 3.0 ml was drawn for UV–visible spectroscopic analysis. The MB and CR samples

were scanned in the UV–visible region with the respective blanks. UV–visible absorption spectra were obtained at 5–min intervals to record the changes in absorbance until the solution became completely colorless.

## 5 Results and discussion

The main aim of this work was to explore the use of a biomaterial, i.e. the tuber of *E. herbacea*, in the synthesis of AgNPs. AgNPs were synthesized by bioreduction of $AgNO_3$ using an aqueous extract of *E. herbacea* tubers. Process parameters such as the concentration of $AgNO_3$, the concentration of the tuber extract and reaction time were optimized. The synthesized AgNPs were characterized using sophisticated analytical methods and evaluated for antimicrobial and catalytic activity.

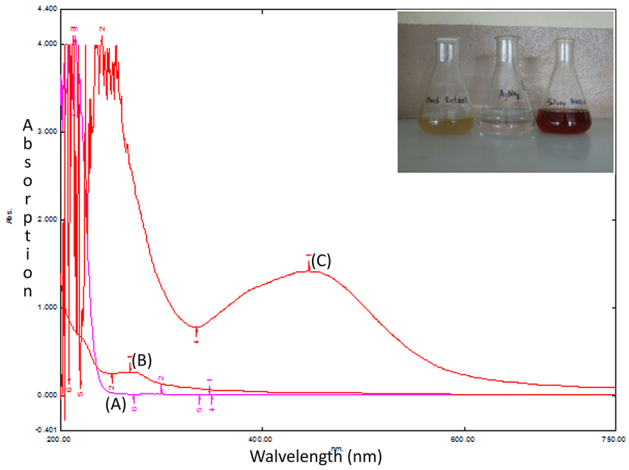


**Fig. 1** UV–visible absorption spectra of **a** $AgNO_3$ solution. **b** *Eulophia herbacea* tuber extract. **c** synthesized AgNPs with absorption maxima at 447 nm

### 5.1 Biosynthesis of AgNPs and characterization

#### 5.1.1 Visual observation and UV–visible spectroscopy study

A colorless solution turning brown is the visual observation that confirms the reduction of the silver salt and the synthesis of AgNPs. The synthesis of the AgNPs (bioreduction of $Ag^+$ to $Ag^0$) was monitored by studying UV–visible absorption spectra of the test sample with respect to time. The increase in absorbance and the color change of the solution with time were noted. The AgNPs absorbance was measured at wavelength 447 nm (Fig. 1). The UV–visible absorption spectra of the $AgNO_3$ solution and the *E. herbacea* tuber extract do not show any absorption at 447 nm (Fig. 1).

The brown coloration was due to surface plasma resonance vibration excitation of the AgNPs [39]. The AgNP solution had a yellowish-brown color with a surface plasma resonance (SPR) absorption maximum at 447 nm, which is the spectral characteristic of AgNPs [47]. There was a red shift in the surface plasma resonance of the AgNPs relative to 420 nm due to adsorption of phytoconstituents of the tuber extract that may act as capping and stabilizing agents of nanoparticles. This confirms the capability of the aqueous extract of the tuber of *E. herbacea* to reduce silver ions to zero-valent silver in the nano form.

#### 5.1.2 Optimization study

An $AgNO_3$ concentration of 1 mM and an *E. herbacea*aqueous tuber extract of 2.5 ml produced the maximum absorption at 447 nm (Fig. 2).

**5.1.2.1 Optimized synthesis of AgNPs** AgNPs were synthesized by adding 2.5 ml of *E. Herbacea* aqueous tuber extract (2% w/v) to 1 mM $AgNO_3$ (10 ml) for 5 h (Fig. 1). This method requires lesser time as compared to earlier reports on AgNPs synthesis using plant extracts [4, 7, 8, 25–27]. Different phytoconstituents were found in the tuber extract (Table 1). The UV–visible spectrum of the resulting AgNP solution was recorded at intervals of 1 h up to 5 h. The maximum absorption was obtained at about 5 h. Different concentrations of $AgNO_3$ with and the extract were scanned in the UV–visible region to optimize the $AgNO_3$ concentration. The deviation in the absorption was studied as a function of the concentration of $AgNO_3$ in the UV–visible region.

With high concentrations of $AgNO_3$ (5 mM, 10 mM) and high extract quantities (3.0 ml, 4.0 ml), the resulting solution had broad peaks of lower intensities. This may be due to agglomeration of nanoparticles, which leads to slow rates of bioreduction [5, 9]. The concentration of $AgNO_3$ has a significant effect on the synthesis of AgNPs. With a tuber extract quantity of 0.5–2.5 ml, an increase in absorption of the resulting nanoparticle solution was observed. This may be due to the different phytoconstituents present in the tuber extract (Table 1).

The phytoconstituents present in the plant extract directly or indirectly influence the reaction kinetics of the AgNP biosynthesis [5]. The phytochemical are responsible for the fast reduction of metal salts [13]. Carbohydrates, flavonoids, saponins, tannins-phenol, and proteins were among the phytoconstituents present in

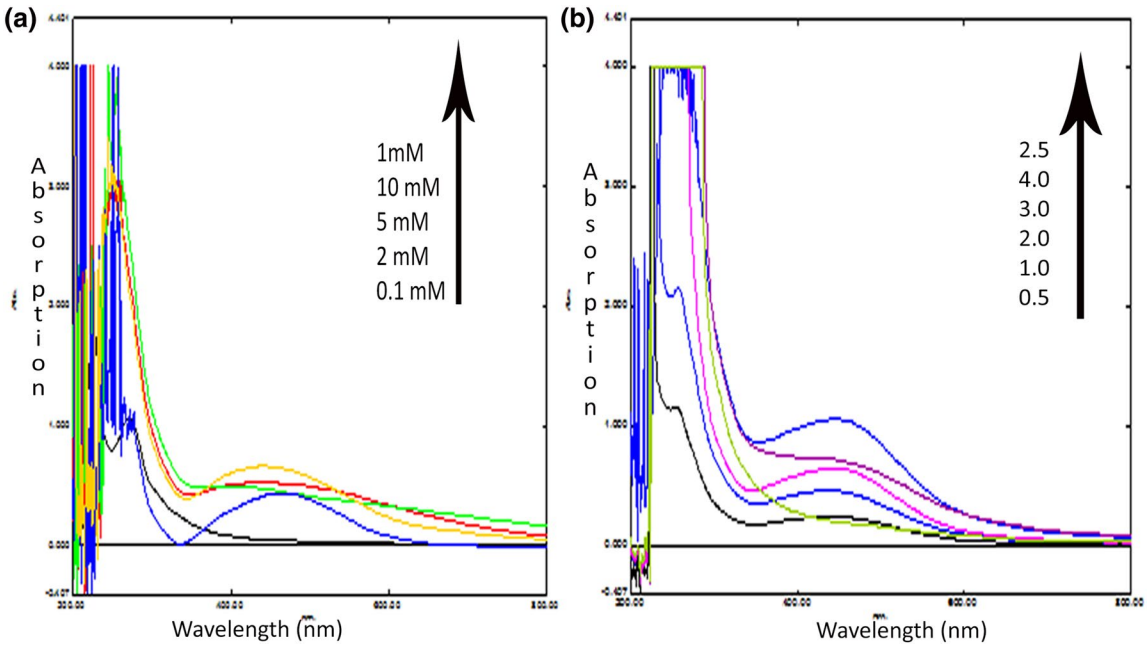


**Fig. 2** **a** UV–visible spectra with different concentrations of $AgNO_3$ with *E. herbecea* tuber extract. **b** UV–visible spectra of different quantity of *E. herbecea* tuber extract solution with 1 mM $AgNO_3$

**Table 1** Phytochemical screening results of *Eulophia herbacea* tuber extract

| Phytochemicals | Chemical tests | *E. herbacea* tuber aqueous extract |
|---|---|---|
| Carbohydrate | Molish test | +++ |
| | Fehling test | +++ |
| | Benedict's test | +++ |
| Flavonoids | Shinoda test | + |
| | Zinc HCL test | + |
| Glycoside | Borntrager's test | – |
| Steroids | Salkowski test | – |
| Saponins | Froth formation test | + |
| Tannins | Ferric chloride test | ++ |
| | Gelatin test | ++ |
| Proteins | Biuret | + |
| | Million's test | + |
| | Ninhydrin test | + |
| Alkaloid | Mayer's | – |
| | Wagner's | – |
| | Dragendorff's | – |

–, Absent; +, present at low concentration; ++, present at moderately concentration; +++, present at high concentration

the *E. herbacea* extract (Table 1), which is consistent with previous reports. The progress of the AgNP synthesis (bioreduction of $Ag^+$ to $Ag^0$) was monitored by studying UV–visible spectra with respect to time.

### 5.1.3 FT-IR analysis

The functional groups responsible for the biosynthesis of the AgNPs were qualitatively determined through FT-IR analysis. The IR peaks of the *E. herbacea* tuber extract were at 521, 814, 877, 908, 956, 1030, 1062, 1093, 1149, 1246, 1377, 1426, 1646, 1728, 2191, 2891, 2947 and 3353 $cm^{-1}$ (Fig. 3a). The observed FT-IR peaks can be assigned to different functional groups: 877 $cm^{-1}$,–C–N stretching; 1030 $cm^{-1}$, –C–O–C stretching; 1149 $cm^{-1}$, Ar–O–C stretching; 1377 and 1426 $cm^{-1}$, –C–H bending; 1646 $cm^{-1}$, C=C stretching, presence of an unsaturated system; 1728 $cm^{-1}$,–C=O stretching; 2891 and 2947 $cm^{-1}$, C–H stretching; 3353 $cm^{-1}$, –NH stretching or bonded –OH. The functional groups determined as being present in the extract were in accordance with the presence of carbohydrates, proteins, saponins and flavonoids in the *E. herbacea* tuber extract as determined by phytochemical testing.

IR peaks of the AgNPs (after bioreduction of $AgNO_3$) were found at 610, 1091, 1240, 1384, 1557, 1656, 2932 and 3324 $cm^{-1}$ (Fig. 3b). The broad peak at 610 $cm^{-1}$ is related to AgNPs bonding with oxygen from the hydroxyl groups of the *E. herbacea* tuber extract. The decrease in peak intensity at 2891 and 2947 $cm^{-1}$ (–C–H stretching) and the absence of a peak at 1728 $cm^{-1}$ (carbonyl stretching) confirm the reduction caused by the

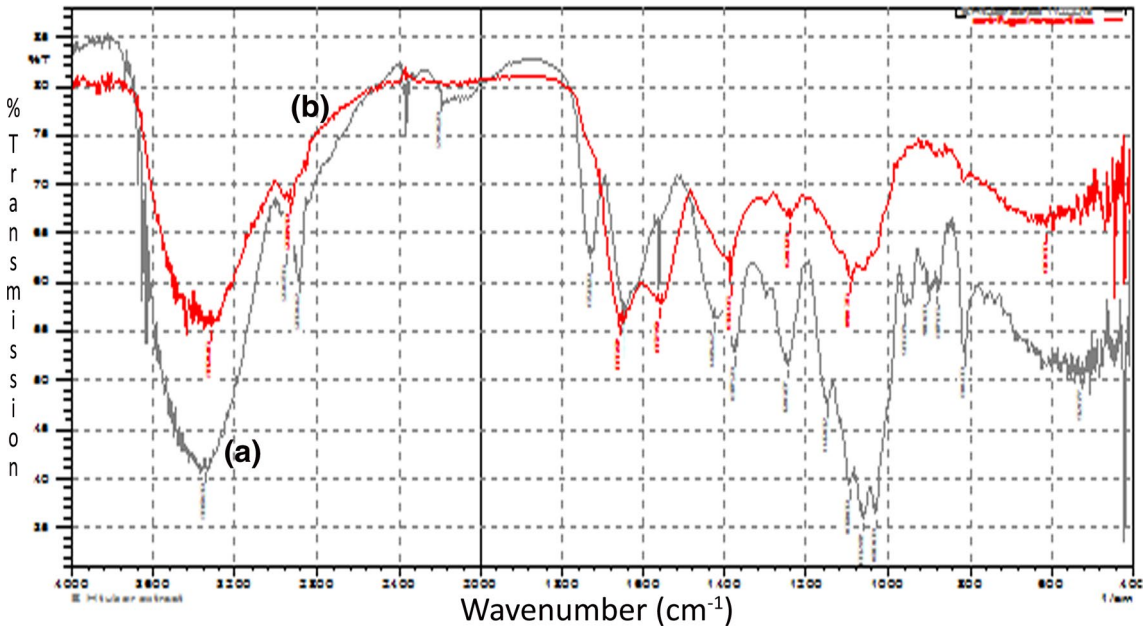


**Fig. 3** FT-IR spectra of **a** Plant tuber extract before reduction. **b** AgNPs after bioreduction

extract. The FT-IR peak at 1557 $cm^{-1}$ was assigned to C–C stretching, and the 1384 $cm^{-1}$ peak was assigned to C–N stretching. These peaks confirm the presence of biomolecules in the AgNPs. Similar peaks are observed with carbohydrates and proteins, and so the presence of these in the AgNPs is indicated. The phytoconstituents act as reducing agents as well as stabilizing and capping agents in the biosynthesis of the nanoparticles. The FT-IR study reveals that the biomolecules present in the *E. herbacea* tuber extract were responsible for reduction and capping in the biosynthesis of the AgNPs.

#### 5.1.4 Particle size analysis and zeta potential

The zeta potential of the AgNPs was found to be − 15.2 mV. The mean particle size of the AgNPs was 37.82 (d nm), with a PdI value of 0.284.

The zeta potential was determined to understand the surface charge of the AgNPs. The negative zeta potential indicates that the AgNPs are fairly stable due to electrostatic repulsion [48, 49]. The size distribution and the average particle size of the nanoparticles were obtained by particle size analysis. The dynamic light scattering (DLS) method, based on laser diffraction with multiple scattering, is used in particle size measurement, and the PdI was determined.

#### 5.1.5 SEM, EDX and X-ray diffraction analysis of AgNPs

The SEM study revealed that the average particle size of the synthesized AgNPs was 11.70 ± 2.43 nm. The AgNPs were not agglomerated (Fig. 4). The EDX spectrum of the synthesized AgNPs shows the intense peaks of Ag, Cl and O (Fig. 5). The reduction of the silver ion to elemental silver was confirmed by the EDX spectrum. The elemental composition of the material (i.e., the inorganic ions present in the samples) was determined using EDX spectroscopy. The Ag signal at 3 keV in the EDX spectrum confirms the

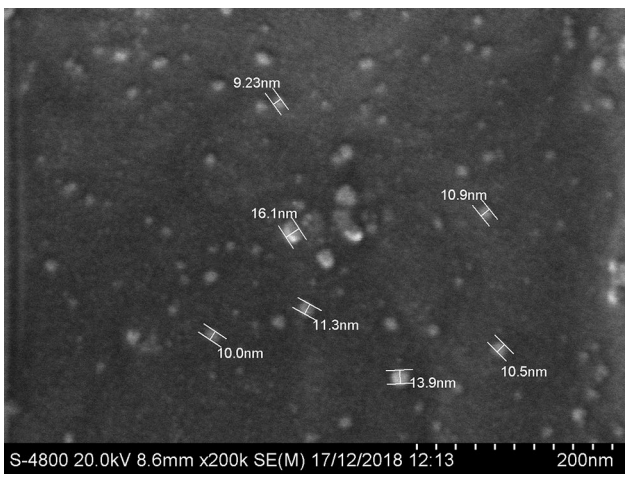


**Fig. 4** SEM of synthesized AgNPs

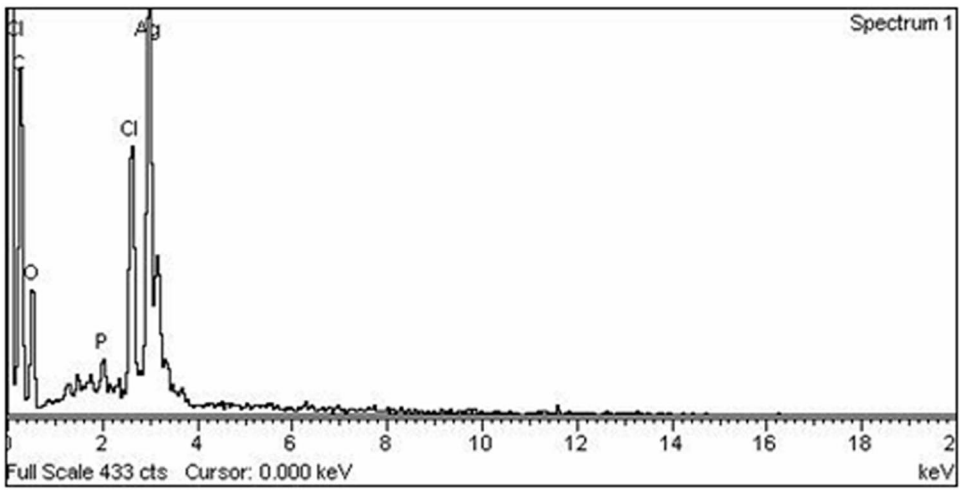


**Fig. 5** EDX spectra of synthesized AgNPs

presence of silver atoms in the AgNPs. This signal is due to surface plasmon resonance [50].

X-ray diffraction peaks were obtained at 2$\theta$ values of 37.24°, 45.37°, 63.7° and 76.05°. The peaks were assigned to the planes (111), (200), (220) and (311) corresponds to the face-centered cubic geometry of the synthesized AgNPs (Fig. 6). The X-ray diffraction study confirms the crystalline nature of the synthesized AgNPs. SEM scanning was performed to understand the morphology of the AgNPs. The X-ray data are in good agreement with Joint Committee for Powder Diffraction Set (JCPDS) Card No. 04-0783.

## 5.2 Biological and catalytic activity of AgNPs

### 5.2.1 Antimicrobial activity of Ag nanoparticles

The antimicrobial activity of the synthesized AgNPs was evaluated by measuring the zone of inhibition against the

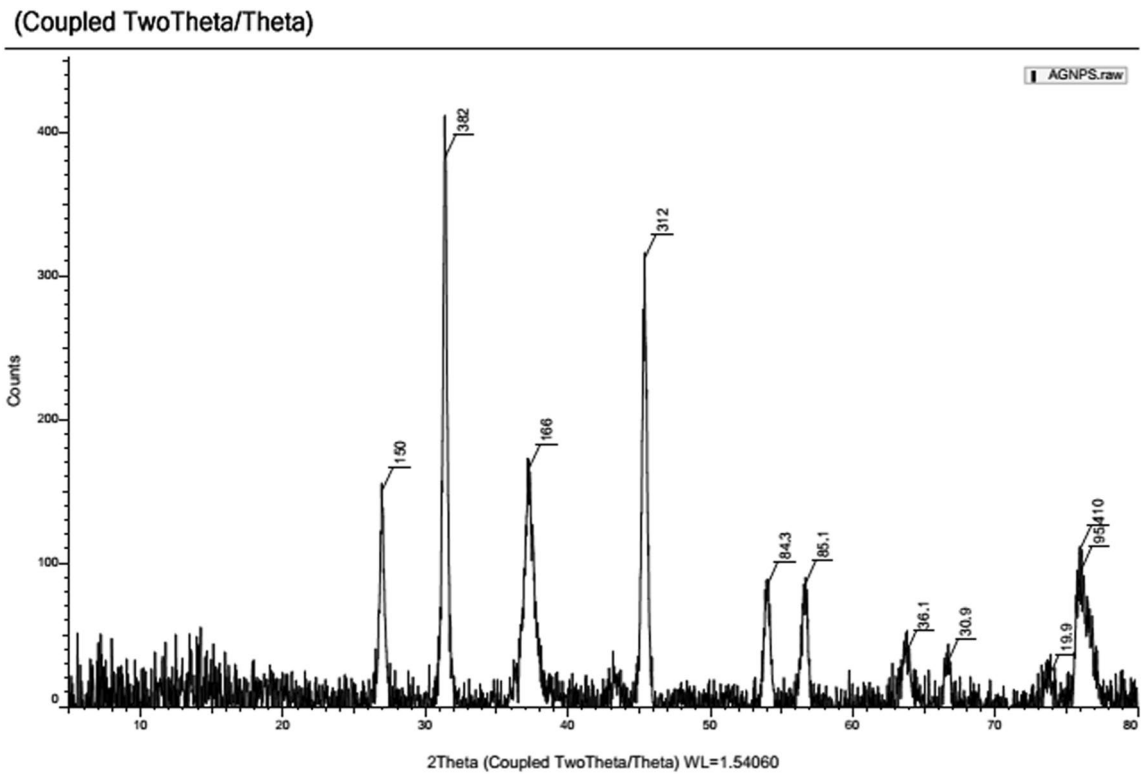


**Fig. 6** Xrd pattern of AgNPs

test organisms: Gram-positive bacteria (*S. aureus, B. subtilis*) and Gram-negative bacteria (*E. coli, P. aeuroginosa*) (Fig. 7, Table 2). The synthesized AgNPs were found to exhibit potent antibacterial activity against both Gram-positive bacteria and Gram-negative bacteria. The synthesized AgNPs exhibited stronger antibacterial activity compared with the corresponding silver nitrate solution and the *E. herbacea* tuber extract. The plant tuber extract (2% w/v) did not show any antibacterial activity against the test organisms. The zones of inhibition of the Gram-positive bacteria (*B. subtilis and S. aureus*) were larger compared with those of the Gram-negative bacteria (*E. coli and P. aeruginosa*).

The minimum inhibitory concentration (MIC) results obtained from the plate assay are shown in Table 2. The antimicrobial MIC values of the AgNPs were found to be

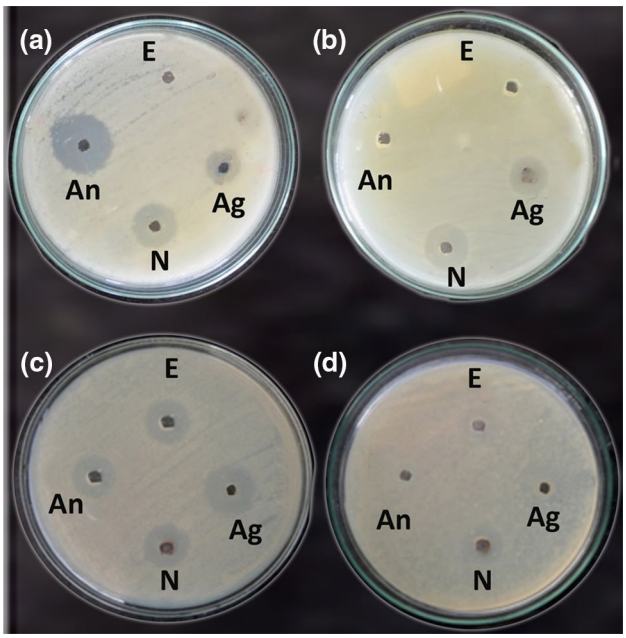


**Fig. 7** **a** Inhibition zones against *B. subtilus* by synthesized AgNPs. **b** Inhibition zones against *P. aeurogenosa* by AgNPs. **c** Inhibition zones against *S. aureus* by AgNPs **d** Inhibition zones against *E. coli* by AgNPs

10 µg/ml for *E. coli*, 10 µg/ml for *S. aureus*, 10 µg/ml for *P. aeuroginosa* and 12.5 µg/ml for *B. subtilis.*

The AgNPs were shown to be an effective bactericide against Gram-positive and Gram-negative bacteria [48]. The AgNPs get attached to the bacterial cell wall, causing structural changes in the cell membrane and leading to death [17]. The Gram-positive bacteria (*B. subtilis* and *S. aureus*) may have had larger zones of inhibition compared with the Gram-negative bacteria (*E. coli and P. aeruginosa*) (Fig. 7) due to differences in the composition of the cell wall. The cell walls of Gram-positive bacteria contain more peptidoglycon than do those of Gram-negative bacteria [51, 52].

#### 5.2.2 Antifungal activity

The results of the antifungal activity study are presented in Fig. 8 and Table 3. The AgNPs exhibited better antifungal activity against *F. moniliforme* compared with *A. niger*. AgNPs penetrate the cell and bind to the DNA of fungi, forming a complex, which leads to inhibition of DNA replication [53, 54]. Several researchers have demonstrated the antibacterial activity of the metal nanoparticles [23–27]. However, a very few reports are available on antifungal activity of the AgNPs.

#### 5.2.3 Synergistic effect of AgNPs with antibiotics

The results of the study of the synergistic activity of the AgNPs along with the antibiotics streptomycin and chloramphenicol are shown in Fig. 9.

The synergistic activity of AgNPs with streptomycin was found to 0.9-fold against *E. coli*, 0.3-fold against *S. aureus*, 0.4-fold against *P. Aeuroginosa* and 0.08-fold against *B. subtilis*. The best synergist activity with streptomycin (0.9-fold) was found against *E. coli*.

The synergistic activity of AgNPs with chloramphenicol was found to 8.61-fold against *E. coli*, 2.24-fold against *S. aureus*, 0.30-fold against *P. aeuroginosa* and 10.11-fold against *B. subtilis*. The best synergist activity with chloramphenicol (10.11-fold) was against

**Table 2** Antibacterial activity of biosynthesized AgNPs

| Microorganisms | Zone of inhibition (mm) ± SD | | | | |
|---|---|---|---|---|---|
| | Silver nitrate (1 mM) | *Eulophia herbacea*aqueous extract (2% w/v) | Silver nanoparticles (20 µg/ml) | Positive control (streptomycin 30 µg/ml) | MIC (µg/ml) |
| *B. subtilus* | 11 ± 0.37 | NI | 16 ± 0.20 | 10 ± 0.61 | 10 |
| *S. aureus* | 12 ± 0.57 | NI | 14 ± 0.50 | 09 ± 0.29 | 10 |
| *E. coli* | 10 ± 0.30 | NI | 12 ± 0.13 | 18 ± 0.57 | 10 |
| *P. aeurogenosa* | 12 ± 0.48 | NI | 13 ± 0.41 | 17 ± 0.70 | 12.5 |

*NI* no inhibition


**Fig. 8** Antifungal activity of AgNPs **a** against *Aspergillus niger*. **b** Against *Fusarium moniliforme*

**Table 3** Antifungal activity of AgNPs

| Microorganisms | Zone of inhibition (mm) ± Standard Deviation | | | |
|---|---|---|---|---|
| | $AgNO_3$ (1 mM) | *Eulophia herbecea* tuber extract (2% w/v) | Ag Nanoparticles (25 µg/ml) | Positive control (Amphotericin B, 30 µg/ml) |
| *A. niger* | 9 ± 0.28 | NI | 11 ± 0.40 | 13 ± 0.44 |
| *Fusarium moniliforme* | 8 ± 0.31 | NI | 14 ± 0.55 | 10 ± 0.31 |

*NI* no inhibition

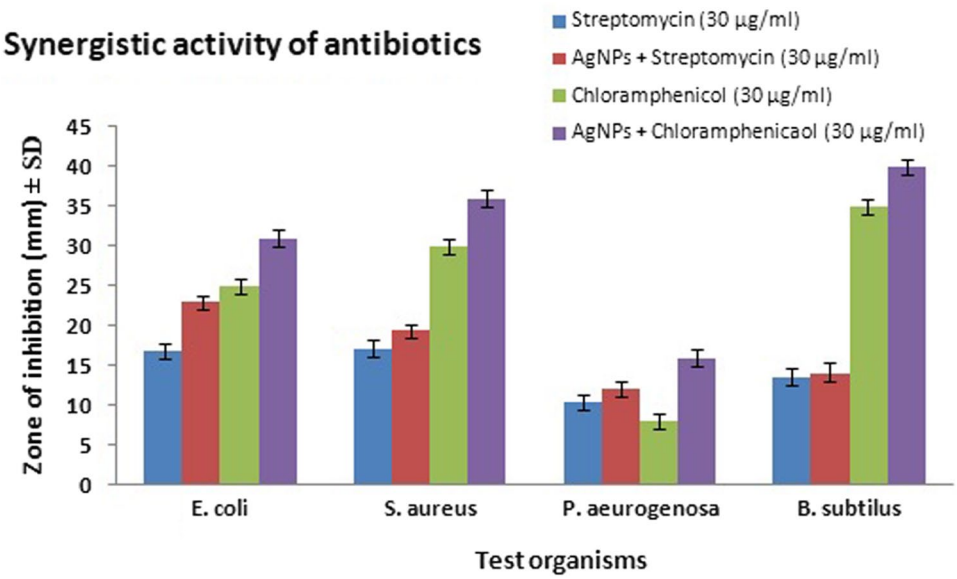


**Fig. 9** Synergistic activity of AgNPs with standard antibiotics

*B. subtilis*. These findings are in good agreement with those of earlier studies [55]. The synergistic effect of synthesized AgNPs with commercial antibiotics is reported here which is promising in treatment of drug-resistant bacteria.

#### 5.2.4 Catalytic activity of AgNPs by reduction of organic dyes

A kinetic study of the reduction of dyes (MB and CR) by $NaBH_4$ was performed in the presence and absence of AgNPs as shown in Fig. 10.

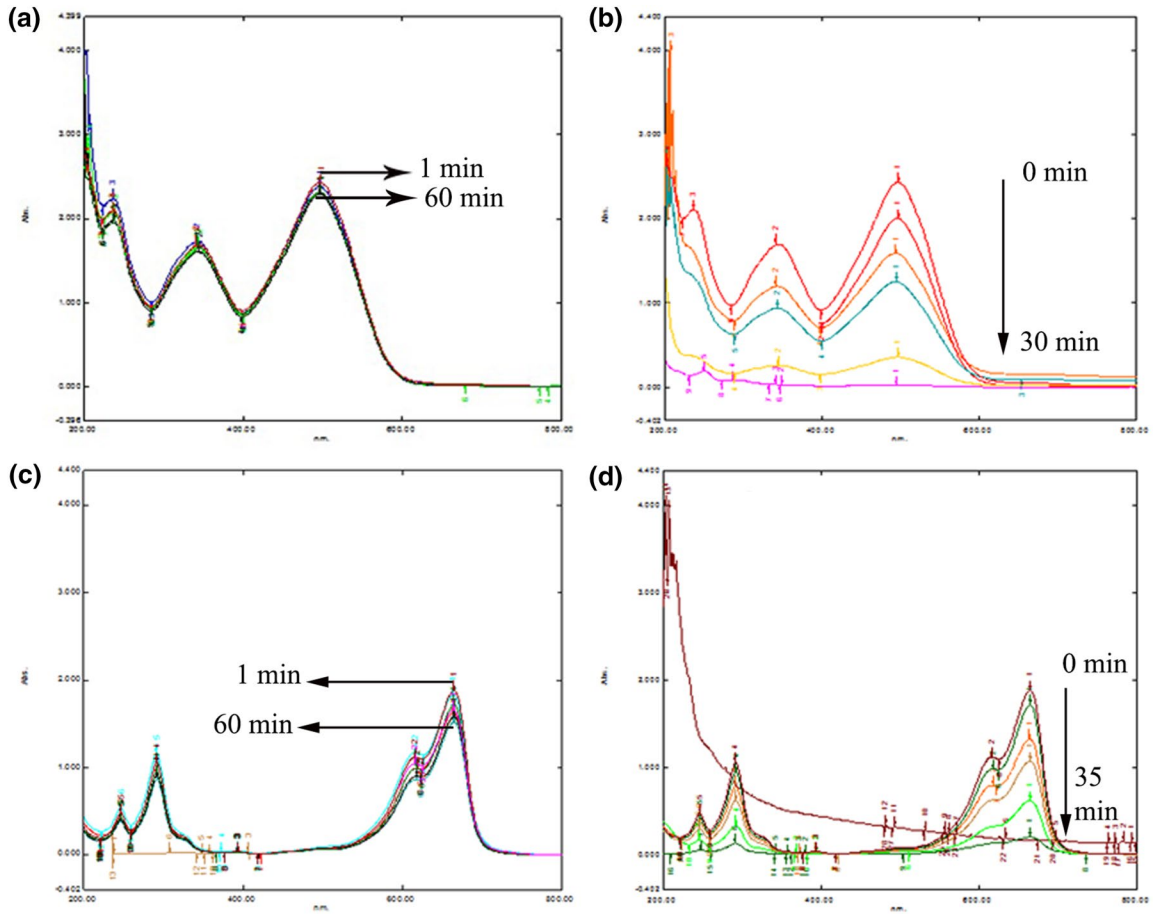


**Fig. 10** Dye reduction activity **a** UV–Vis spectrum of MB reduction by $NaBH_4$ in the absence of AgNPs for a period of 60 min in 5 min interval. **b** UV–Vis spectrum of MB catalytic reduction by $NaBH_4$ in the presence of AgNPs for a period of 30 min in 5 min interval. **c** UV–Vis spectrum of CR reduction by $NaBH_4$ in the absence of AgNPs for a period of 60 min in 5 min interval. **d** UV–Vis spectrum of CR reduction by $NaBH_4$ in the presence of AgNPs for a period of 60 min in 5 min interval

The capability of the synthesized AgNPs to reduce MB and CR was assessed at varying time intervals through the absorption in the UV–visible region. The maximum absorption of MB in the UV–visible region was at a wavelength of 664 nm and that of CR was at 338 mm and 498 nm. In the absence of AgNPs, the rates of reduction of MB and CR by $NaBH_4$ are very slow and the reaction was never completed. $NaBH_4$ and the AgNPs were individually not capable of degrading the dyes.

In the presence of AgNPs (7 µg/ml), $NaBH_4$ was capable of reducing the dyes. The absorption of the dyes was decreased gradually against time due to interaction with the AgNPs. The reduction reaction rate was increased and the reaction was close to completion after 30 min. The synthesized AgNPs by *E. Herbacea* tuber extract acted as a catalyst, increasing the rate of reduction of methylene blue and Congo red. The earlier methods of AgNPs synthesis by tubers were limited to biological activities and does not explored dye reduction studies [4, 7, 8]. The maximum absorption of MB (a thiazine dye) in the UV–visible region was at a wavelength of 664 nm and that of CR (an azo dye) was at 338 mm and 498 nm. MB and CR are non-biodegradable. Azo dyes are mostly used in the dye industry and are one of the sources of water pollution. The catalytic reduction of MB and CR was investigated by using $NaBH_4$ as a reducing agent in the presence of an AgNP catalyst. At high concentrations of $NaBH_4$ compared with the dye concentration, the degradation of $BH_4^-$ ions was retarded due increase in pH of reaction mixture which hinder aerial oxidation of reduced dyes products. In the presence of AgNPs, the transfer of electrons from the $BH_4^-$ species (electron donor species) to dyes (MB and CR, i.e., electron acceptor species) was carried out effectively, leading to a decrease in the activation energy and stabilization of the system. The rate of the reduction reaction was assumed to be independent of the $NaBH_4$ concentration as much more of it was present compared with the dyes. For AgNPs, the $BH_4^-$ ions (as nucleophilic) whereas dyes as electrophilic in

nature. In the presence of $NaBH_4$, the AgNPs help transfer the electrons from $BH_4^-$ ions to the azo bonds in the dyes. This study indicates the role of AgNPs as a catalyst in the process of reduction of dyes as compared to earlier reports of tuber [4, 7]. So AgNPs biosynthesized from an extract of the tuber of *E. herbecea* can be used to remove MB and CR from wastewater.

## 6 Conclusion

Simple, cost-effective and eco-friendly phytochemical synthesis of AgNPs using *E. herbacea* tuber extract was reported. The phytochemicals present in the tuber extract played a significant role in the bioreduction and stabilization of the synthesized AgNPs. The synthesized AgNPs were characterized by UV–Vis, FT-IR, SEM, EDX and X-ray diffraction spectroscopy. The SEM study revealed that the average particle size of the synthesized AgNPs was $11.70 \pm 2.43$ nm and that the nanoparticles were non-agglomerated. The synthesized AgNPs displayed antibacterial activity (against both Gram-negative and Gram-positive bacteria) and antifungal activity. The AgNPs displayed synergistic activity in combination with antibiotics. The synthesized AgNPs were capable of reducing organic dyes such as MB and CR within 60 min, and this indicates their catalytic activity.

**Acknowledgement** The authors thank KBC North Maharashtra University, Jalgaon and UGC-DAE Consortium for Scientific Research, Indore Centre, University Campus, Khandwa Road, Indore 452017, India, for allowing them to carry out SEM and EDX analysis of the metal nanoparticles.

**Author contributions** All authors contributed to the study conception and design. The work was designed by Jayashri S. Pawar and Ravindra H. Patil. The experimental work was done by Jayashri S. Pawar whereas analyses of results were done by Jayashri S. Pawar and Ravindra H. Patil. The manuscript was written by Jayashri S. Pawar and Ravindra H. Patil. All authors read and approved the final manuscript.

**Availability of data and material** The datasets used and/or analysed during the current study are available from the corresponding author on reasonable request.

### Compliance with ethical standards

**Conflict of interest** The authors declare that they have no conflict of interest.

## References

1. Mittal AK, Chisti Y, Banerjee UC (2013) Synthesis of metallic nanoparticles using plant extracts. Biotechnol Adv 31(2):346–356
2. Sathishkumar M, Sneha K, Yun Y-S (2013) Green fabrication of zirconia nano-chains using novel *Curcuma longa* tuber extract. Mater Lett 98:242–245
3. Kharissova OV, Dias HR, Kharisov BI, Pérez BO, Pérez VMJ (2013) The greener synthesis of nanoparticles. Trends Biotechnol 31(4):240–248
4. Shameli K, Ahmad MB, Zamanian A, Sangpour P, Shabanzadeh P, Abdollahi Y, Zargar M (2012) Green biosynthesis of silver nanoparticles using *Curcuma longa* tuber powder. Int J Nanomed 7:5603
5. Maria BS, Devadiga A, Kodialbail VS, Saidutta M (2015) Synthesis of silver nanoparticles using medicinal *Zizyphus xylopyrus* bark extract. Appl Nanosci 5(6):755–762
6. Alam MN, Roy N, Mandal D, Begum NA (2013) Green chemistry for nanochemistry: exploring medicinal plants for the biogenic synthesis of metal NPs with fine-tuned properties. RSC Adv 3(30):11935–11956
7. Sathishkumar M, Sneha K, Yun Y-S (2010) Immobilization of silver nanoparticles synthesized using *Curcuma longa* tuber powder and extract on cotton cloth for bactericidal activity. Biores Technol 101(20):7958–7965
8. Sivakumar T, Gajalakshmi D, Subramanian V, Palanisamy K (2015) Tuber extract mediated biosynthesis of silver nanoparticles and its antioxidant, antibacterial activity. J Biol Sci 15:68
9. Ghosh S, Patil S, Ahire M, Kitture R, Kale S, Pardesi K, Cameotra SS, Bellare J, Dhavale DD, Jabgunde A (2012) Synthesis of silver nanoparticles using *Dioscorea bulbifera* tuber extract and evaluation of its synergistic potential in combination with antimicrobial agents. Int J Nanomed 7:483
10. Nagajyothi P, Lee K (2011) Synthesis of plant-mediated silver nanoparticles using *Dioscorea batatas* rhizome extract and evaluation of their antimicrobial activities. J Nanomater 2011:49
11. Maheswari R, Prabha AL, Nandagopalan V, Anburaja V (2012) Green synthesis of silver nanoparticles by using rhizome extract of *Dioscorea oppositifolia* L. and their anti microbial activity against human pathogens. J Pharm Biol Sci 1:38–42
12. Panáček A, Kvítek L, Prucek R, Kolář M, Večeřová R, Pizúrová N, Sharma VK, Tj Nevěčná, Zbořil R (2006) Silver colloid nanoparticles: synthesis, characterization, and their antibacterial activity. J Phys Chem B 110(33):16248–16253
13. Prabhu S, Poulose EK (2012) Silver nanoparticles: mechanism of antimicrobial action, synthesis, medical applications, and toxicity effects. Int Nano Lett 2(1):32
14. Huang J, Zhan G, Zheng B, Sun D, Lu F, Lin Y, Chen H, Zheng Z, Zheng Y, Li Q (2011) Biogenic silver nanoparticles by *Cacumen platycladi* extract: synthesis, formation mechanism, and antibacterial activity. Ind Eng Chem Res 50(15):9095–9106
15. Manosalva N, Tortella G, Diez MC, Schalchli H, Seabra AB, Durán N, Rubilar O (2019) Green synthesis of silver nanoparticles: effect of synthesis reaction parameters on antimicrobial activity. World J Microbiol Biotechnol 35(6):88
16. Dakal TC, Kumar A, Majumdar RS, Yadav V (2016) Mechanistic basis of antimicrobial actions of silver nanoparticles. Frontiers Microbiol 7:1831
17. Sondi I, Salopek-Sondi B (2004) Silver nanoparticles as antimicrobial agent: a case study on *E. coli* as a model for Gram-negative bacteria. Journal of colloid and interface science 275(1):177–182
18. Kim JS, Kuk E, Yu KN, Kim J-H, Park SJ, Lee HJ, Kim SH, Park YK, Park YH, Hwang C-Y (2007) Antimicrobial effects of silver nanoparticles. Nanomed Nanotechnol Biol Med 3(1):95–101
19. Feng QL, Wu J, Chen G, Cui F, Kim T, Kim J (2000) A mechanistic study of the antibacterial effect of silver ions on *Escherichia coli* and *Staphylococcus aureus*. J Biomed Mater Res 52(4):662–668

20. Matsumura Y, Yoshikata K, Kunisaki S-i, Tsuchido T (2003) Mode of bactericidal action of silver zeolite and its comparison with that of silver nitrate. Appl Environ Microbiol 69(7):4278–4281
21. Morones JR, Elechiguerra JL, Camacho A, Holt K, Kouri JB, Ramírez JT, Yacaman MJ (2005) The bactericidal effect of silver nanoparticles. Nanotechnology 16(10):2346
22. Hatchett DW, White HS (1996) Electrochemistry of sulfur adlayers on the low-index faces of silver. J Phys Chem 100(23):9854–9859
23. Fayaz AM, Balaji K, Girilal M, Yadav R, Kalaichelvan PT, Venketesan R (2010) Biogenic synthesis of silver nanoparticles and their synergistic effect with antibiotics: a study against gram-positive and gram-negative bacteria. Nanomed Nanotechnol Biol Med 6(1):103–109
24. Bhakya S, Muthukrishnan S, Sukumaran M, Muthukumar M, Kumar ST, Rao M (2015) Catalytic degradation of organic dyes using synthesized silver nanoparticles: a green approach. J Bioremed Biodegred 6(5):1
25. Indana MK, Gangapuram BR, Dadigala R, Bandi R, Guttena V (2016) A novel green synthesis and characterization of silver nanoparticles using gum tragacanth and evaluation of their potential catalytic reduction activities with methylene blue and Congo red dyes. J Anal Sci and Technol 7(1):19
26. Ganapuram BR, Alle M, Dadigala R, Dasari A, Maragoni V, Guttena V (2015) Catalytic reduction of methylene blue and Congo red dyes using green synthesized gold nanoparticles capped by salmalia malabarica gum. Int Nano Lett 5(4):215–222
27. Seralathan J, Stevenson P, Subramaniam S, Raghavan R, Pemaiah B, Sivasubramanian A, Veerappan A (2014) Spectroscopy investigation on chemo-catalytic, free radical scavenging and bactericidal properties of biogenic silver nanoparticles synthesized using *Salicornia brachiata* aqueous extract. Spectrochim Acta Part A Mol Biomol Spectrosc 118:349–355
28. Nanaei M, Nasseri MA, Allahresani A, Kazemnejadi M (2019) *Phoenix dactylifera* L. extract: antioxidant activity and its application for green biosynthesis of Ag nanoparticles as a recyclable nanocatalyst for 4-nitrophenol reduction. SN Appl Sci 1(8):853
29. Patil DA (1992) Flora of Dhule and Nandurbar District. Bishan Singh and Mahender Pal Singh Publication, Dehradhun
30. Tatiya A, Surana S, Bhavsar S, Patil D, Patil Y (2012) Pharmacognostic and preliminary phytochemical investigation of *Eulophia herbacea* Lindl. Tubers (Orchidaceae). Asian Pac J Trop Dis 2:S50–S55
31. Patil DA, Patil SL (2007) Ethanomedical plants of Dhule districts, Maharashtra. Nat Prod Radiance 6:148–151
32. Tatiya AU, Puranik PM, Surana SJ, Patil YS, Mutha RE (2013) Evaluation of hypolipidemic, antidiabetic and antioxidant activity of Eulophia herbacea tubers. Bangladesh J Pharmacol 8(3):269–275
33. Tamer C, Karaman B, Copur O (2006) traditional Turkish beverage: salep. Food reviews international
34. Chua M, Baldwin TC, Hocking TJ, Chan K (2010) Traditional uses and potential health benefits of *Amorphophallus konjac* K. Koch ex N.E.Br. J Ethnopharmacol 128(2):268–278. https://doi.org/10.1016/j.jep.2010.01.021
35. Khare CP (2007) Indian medicinal plants: an illustrated dictionary. Spring, LLC
36. Dogan M, Kayacier A (2004) Rheological properties of reconstituted hot salep beverage. Int J Food Prop 7(3):683–691
37. Kokate CKPA, Gokhale SB (2009) Pharmacognosy. Nirali Prakashan, Pune
38. Khandelwal K (2006) Practical pharmacognosy, sixteen edn. Nirali Prakashan, Pune
39. Singh K, Panghal M, Kadyan S, Yadav JP (2014) Evaluation of antimicrobial activity of synthesized silver nanoparticles using *Phyllanthus amarus* and *Tinospora cordifolia* medicinal plants. J Nanomed Nanotechnol 5(6):1
40. Awwad AM, Salem NM, Abdeen AO (2013) Green synthesis of silver nanoparticles using carob leaf extract and its antibacterial activity. Int J Ind Chem 4(1):29
41. Perz C, Paul M, Bazerque P (1990) An antibiotic assay by the agar well diffusion method. Acta Biol Med Exp 15:113–115
42. Maiti S, Krishnan D, Barman G, Ghosh SK, Laha JK (2014) Antimicrobial activities of silver nanoparticles synthesized from *Lycopersicon esculentum* extract. J Anal Sci Technolgy 5(1):40
43. Satish S, Raghavendra M, Raveesha K (2008) Evaluation of the antibacterial potential of some plants against human pathogenic bacteria. Adv Biol Res 2(3–4):44–48
44. Bhimba JSDBV (2014) Antibacterial and antifungal activity of silver nanoparticles synthesized using Hypnea muciformis. Biosci Biotechnol Res Asia 11(1):235–238
45. Rahim KAAA, Mohamed AMA (2015) Bactericidal and antibiotic synergistic effect of nanosilver against methicillin-resistant Staphylococcus aureus. Jundishapur J Microbiol 8(11):e25867
46. Suvith V, Philip D (2014) Catalytic degradation of methylene blue using biosynthesized gold and silver nanoparticles. Spectrochim Acta Part A Mol Biomol Spectrosc 118:526–532
47. Burda C, Chen X, Narayanan R, El-Sayed MA (2005) Chemistry and properties of nanocrystals of different shapes. Chem Rev 105(4):1025–1102
48. Patil Shriniwas P (2017) Antioxidant, antibacterial and cytotoxic potential of silver nanoparticles synthesized using terpenes rich extract of *Lantana camara* L. leaves. Biochemistry and biophysics reports 10:76
49. Bunghez I, Barbinta Patrascu M, Badea N, Doncea S, Popescu A, Ion R (2012) Antioxidant silver nanoparticles green synthesized using ornamental plants. J Optoelectron Adv Mater 14(11):1016
50. Kaviya S, Santhanalakshmi J, Viswanathan B, Muthumary J, Srinivasan K (2011) Biosynthesis of silver nanoparticles using *Citrus sinensis* peel extract and its antibacterial activity. Spectrochim Acta Part A Mol Biomol Spectrosc 79(3):594–598
51. Ankanna S, Prasad TNVKV, Elumalai E, Savithramma N (2010) Production of biogenic silver nanoparticles using *Boswellia ovalifoliolata* stem bark. Dig J Nanomater Biostruct 5(2):369–372
52. Maliszewska I, Sadowski Z (2009) Synthesis and antibacterial activity of of silver nanoparticles. J Phys Conf Ser 1:012024
53. Kolya H, Maiti P, Pandey A, Tripathy T (2015) Green synthesis of silver nanoparticles with antimicrobial and azo dye (Congo red) degradation properties using *Amaranthus gangeticus* Linn leaf extract. J Anal Sci Technol 6(1):33
54. Nasrollahi A, Pourshamsian K, Mansourkiaee P (2011) Antifungal activity of silver nanoparticles on some of fungi. Int J Nano Dimens 1(3):233–239
55. Shahverdi AR, Fakhimi A, Shahverdi HR, Minaian S (2007) Synthesis and effect of silver nanoparticles on the antibacterial activity of different antibiotics against *Staphylococcus aureus* and *Escherichia coli*. Nanomed Nanotechnol Biol Med 3(2):168–171